

## Does flow variance affect bedload flux when the bed is dominated by grain roughness?

James R. Cooper\*

Department of Geography, University of Sheffield, Sheffield, S10 2TN, UK

### ARTICLE INFO

#### Article history:

Received 3 March 2011

Received in revised form 20 December 2011

Accepted 23 December 2011

Available online 31 December 2011

#### Keywords:

Grain roughness

Near-bed flow

Bedload transport

Spatial flow variability

Water-worked gravel beds

Laboratory flume

### ABSTRACT

Previous studies have shown that spatial variance in fluid and critical shear stress, caused by form roughness, can increase bedload flux. Others have revealed that variance in flow velocity increases with relative submergence and that bed mobility is reduced at lower submergences. The paper explores the link between these observations and addresses the following questions: is grain roughness sufficient to cause variance in fluid shear stress and an increase in bedload flux; if this variance changes with submergence, does this mean that the increase is dependent on submergence; and does this explain the change in mobility with submergence? A simple, statistical bedload model, based on spatial distributions of fluid and critical shear stress, has been used to explore these effects over a water-worked gravel deposit. Estimates of spatially distributed fluid shear stress were gained from laboratory flume measurements of near-bed flow velocity, and a distribution of critical shear stress was simulated using a discrete particle model of the sediment distribution used in the flume. The velocity data were used to describe the change in the spatial distribution of near-bed velocity with relative submergence, which allowed the effects of submergence on flux to also be considered. The main conclusions were: (i) spatial variance in fluid shear stress from grain roughness was not sufficient to have an appreciable effect on bedload flux over water-worked gravel beds with a spatial distribution of critical shear stress; (ii) spatial variance in critical shear stress, caused by grain roughness, had a much larger influence and increased bedload flux. This was a similar level of increase observed in studies for conditions where form roughness was high; (iii) spatially averaged estimates of fluid and critical shear stress should not be used to estimate bedload flux even if form roughness is low; and (iv) a rise in relative submergence increased bedload flux. This was due to changes in the spatial distribution of near-bed velocity and not due to a lowering in the local flow velocity as has been suggested by previous studies.

© 2011 Elsevier B.V. All rights reserved.

### 1. Introduction

Bedload transport is a controlling factor in the morphological change of gravel-bed rivers. It is a nonlinear process so the bedload flux within a river depends not only on the mean values of fluid and critical shear stress but also on their spatial variances. In gravel-bed rivers, the surface of a water-worked sediment deposit is spatially complex and highly three-dimensional because of the presence of bedforms occurring at different roughness scales. Commonly fluid shear stress is subdivided into two components: (i) the shear stress caused by the resistance of grains (grain roughness); and (ii) the stress caused by the resistance of the form of the river bed (form roughness). It is well established that grain roughness, caused by things like grain shape, orientation, exposure, sorting, packing and protrusion, controls the distribution of critical shear stress at this granular scale (e.g., [Wiberg and Smith, 1987](#); [Kirchner et al., 1990](#);

[Buffington et al., 1992](#)). Less is known about the spatial variance in fluid shear stress, which occurs because of this grain roughness, and its effect on bedload flux. Up until now, focus has been on examining the influence of form roughness on the variance in fluid shear stress and how this affects bedload flux.

For example, [Ferguson \(2003\)](#) developed an analytical model to quantify the effect of lateral variability in fluid shear stress, caused by changes in channel planform, on bedload transport capacity. He examined its influence on bedload flux for beds with and without spatial variability in critical shear stress. The lateral variability was simulated by using a statistical model that described a theoretical probability distribution for the lateral distribution of shear stress. This allowed both the mean and variance of the distributions to be changed, allowing different degrees of lateral variability in fluid shear stress to be applied. He found that the bedload flux was considerably greater when a lateral variation in fluid shear stress was present, such that bedload flux increased with the variance of fluid shear stress. He showed that lateral variability in fluid shear stress can produce bedload fluxes more than five times greater than those predicted for an invariant fluid shear stress. In a similar fashion,

\* Tel.: +44 114 222 7989; fax: +44 114 222 7907.

E-mail address: [j.cooper@sheffield.ac.uk](mailto:j.cooper@sheffield.ac.uk).

Paola (1996) outlined a model of flow and bedload transport for braided rivers. He used the spatial probability distribution of flow depth as a surrogate measure of the distribution of fluid shear stress. His model showed, if fluid shear stress is assumed to be invariant, bedload transport calculations will underestimate bedload flux by a factor of around three. Nicholas (2000) further developed this model to account for the relationship between flow discharge and the distribution of flow depth at a cross section of a braided river. The revised model showed that lateral variability in fluid shear stress exerts the most influence on bedload flux at low flows, in which bedload fluxes were two to three times greater than those predicted with invariant fluid shear stress. All previous attempts to quantify the effect of spatial variance in fluid shear stress on bedload flux have not been based on velocity measurements.

For beds without any notable form roughness, studies have revealed that the flow is also spatially heterogeneous. For example, low-speed wall streaks, near-wall region bursts (ejections and sweeps), and large-scale flow structures occupying the whole flow depth have been described (e.g., Grass and Mansour-Tehrani, 1996; Shvidchenko and Pender, 2001; Hardy et al., 2009). Also significant spatial variability in time-averaged velocity has been observed (e.g., Lawless and Robert, 2001; Mignot et al., 2009) and shown to have an effect on the fluid shear stress distribution (e.g., Aberle et al., 2008; Cooper and Tait, 2010).

The spatial structure of the flow field is dependent on relative submergence (ratio of flow depth to roughness length scale). This has been observed at the grain scale, as well as at the patch and reach scales. Measurements both in the laboratory and in the field have shown that large-scale flow structures scale with flow depth: their length is typically three to five flow depths, and they have a width and height that is more or less equal to one flow depth (Shvidchenko and Pender, 2001; Roy et al., 2004). An increase in flow depth has also been shown to increase the degree of spatial variability in the turbulent (Lamarre and Roy, 2005; Buffin-Bélanger et al., 2006) and time-averaged properties of the flow (Clifford, 1996; Buffin-Bélanger et al., 2006), as well as influence its spatial structure (Lamarre and Roy, 2005; Legleiter et al., 2007; Cooper and Tait, 2008; Hardy et al., 2009). This led some to conclude that flow depth has a strong control on flow structure in gravel-bed rivers (Roy et al., 2004; Lamarre and Roy, 2005; Legleiter et al., 2007).

Relative submergence also has an important influence on the mobility of a gravel bed. A number of studies have highlighted that the mean fluid shear stress at which sediment is entrained is positively correlated to channel slope (e.g., Ashida and Bayazit, 1973; Bathurst et al., 1983; 1987; Shvidchenko and Pender, 2000; Mueller et al., 2005; Pender et al., 2007; Lamb et al., 2008; Parker et al., 2011). The reduced mobility on steep slopes has been attributed to a lower relative submergence (e.g., Buffington and Montgomery, 1997; Shvidchenko and Pender, 2000; Mueller et al., 2005; Lamb et al., 2008; Parker et al., 2011), and not to changes in form roughness (Mueller et al., 2005; Parker et al., 2011) or increased drag from channel walls and morphologic structures (Lamb et al., 2008). The correlation can exist when only grain roughness dominates. Studies have suggested that this occurs because a lower relative submergence causes a decrease in local flow velocity around bed particles (Ashida and Bayazit, 1973; Graf, 1991; Lamb et al., 2008). This has yet to be confirmed with velocity measurements.

In short, evidence exists that (i) spatial variance in fluid shear stress, caused by form roughness, influences bedload transport capacity; (ii) variance in flow velocity is present at the grain scale; (iii) its distribution and magnitude change with relative submergence; (iv) relative submergence affects bed mobility when only grain roughness dominates; and (v) that grain-scale changes in near-bed flow velocity could cause this change in mobility. No study has explored how this evidence links together and so a number of important questions remain unanswered: (i) is grain roughness sufficient to cause variance

in fluid shear stress and an increase in bedload flux in a similar manner to form roughness; (ii) if this variance changes with submergence, does this also mean that the increase is dependent on submergence; and (iii) does this explain the change in mobility?

This paper attempts to address these questions. A series of laboratory tests were performed over a water-worked gravel bed in which spatially distributed velocity measurements were made of the near-bed flow field. The bed had no notable form roughness elements and was dominated by granular roughness. By carrying out the velocity measurements at various flow depths, the effect of relative submergence on the near-bed velocity distribution was sought. A discrete particle model (DPM) was used to simulate a spatial distribution of critical shear stress for the sediment deposit used in the laboratory experiments. These data are incorporated into a simple, statistical bedload transport model that allows the effects of variance in fluid and critical shear stress, as well as relative submergence, on bedload flux to be isolated. The aim of the paper is to (i) describe the change in the spatial probability distribution of time-averaged velocity with relative submergence; (ii) estimate how these changes in flow influence bedload flux; (iii) estimate how relative submergence affects bedload flux; and (iv) understand how variance in critical shear stress affect the results in (ii) and (iii).

## 2. Methodology

### 2.1. Experimental setup

The tests were conducted in an 18.3 m-long, 0.5 m-wide laboratory flume, with a working length of 15 m, which could be tilted to produce a range of flume slopes. A mixture with a log-normal, unimodal grain size distribution ( $0.15 \text{ mm} < D < 14 \text{ mm}$ ;  $D_{16} = 3.50 \text{ mm}$ ;  $D_{50} = 4.97 \text{ mm}$ ;  $D_{84} = 7.00 \text{ mm}$ ) was used to produce a water-worked gravel deposit. This was formed by feeding material into running water, with the feed rate being twice the estimated transport capacity of the flow. Further details on this methodology and the surface topography of the bed can be found in Cooper and Tait (2009). Briefly, the bed was water-worked and dominated by granular roughness with no notable form roughness elements (standard deviation = 2.14 mm; range = 15.2 mm; skewness = 0.10; kurtosis = 2.84). At the granular scale, the particles were well imbricated, and an abundance of particle clusters along the whole length of the deposit were evident. The bed had a number of properties that closely resembled those found for natural water-worked gravel beds that are dominated by grain roughness: (i) the distributions of the bed surface elevations were positively skewed; (ii) the vertical roughness length scales were less than half the horizontal roughness length scales, i.e., the grain roughness scales were appropriately scaled; (iii) the two-dimensional structure function displayed two distinct regions: a scaling region at small spatial lags and a saturation region at large scales; (iv) the contour plots of the two-dimensional structure function revealed an elliptical shape that extends to scales several times the median grain diameter, indicating the presence of grain-scale sedimentary structures and an anisotropic bed structure; and (v) preferential particle orientation and direction of imbrication in the subsurface, as well as bulk porosity and hydraulic conductivity values that closely resemble those found in poorly sorted gravel lithofacies of in-channel fluvial deposits. This showed that the fed bed was able to simulate, in a simplified manner, both the grain roughness and subsurface properties of established gravel-bed river deposits.

A total of 11 tests were carried out using a range of bed slopes and relative submergences (Table 1) over the same bed. The selected flow conditions were below those required for sediment movement so the bed surface topography did not change during each test. This was so that the adjustment in the velocity distributions was attributable purely to changes in relative submergence rather than surface topography. For each experimental run, a steady flow rate was introduced

**Table 1**  
A summary of the experimental conditions<sup>a</sup>.

| Run | S       | Q (m <sup>3</sup> /s) | h (m)  | h/k | $\tau_0$ (N/m <sup>2</sup> ) | Re     |
|-----|---------|-----------------------|--------|-----|------------------------------|--------|
| 1   | 0.00285 | 0.0016                | 0.0181 | 1.2 | 0.47                         | 2427   |
| 2   | 0.00285 | 0.0039                | 0.0286 | 1.9 | 0.72                         | 5933   |
| 3   | 0.00285 | 0.0064                | 0.0395 | 2.6 | 0.95                         | 9680   |
| 4   | 0.00285 | 0.0087                | 0.0484 | 3.2 | 1.13                         | 13,246 |
| 5   | 0.00285 | 0.0140                | 0.0628 | 4.1 | 1.40                         | 21,339 |
| 6   | 0.00285 | 0.0280                | 0.0900 | 5.9 | 1.85                         | 42,618 |
| 7   | 0.00375 | 0.0162                | 0.0635 | 4.2 | 1.86                         | 24,750 |
| 8   | 0.00465 | 0.0123                | 0.0492 | 3.2 | 1.87                         | 18,720 |
| 9   | 0.00555 | 0.0098                | 0.0399 | 2.6 | 1.87                         | 14,905 |
| 10  | 0.00645 | 0.0069                | 0.0335 | 2.2 | 1.87                         | 10,546 |
| 11  | 0.00735 | 0.0065                | 0.0295 | 1.9 | 1.90                         | 9977   |

<sup>a</sup> S is the bed slope, Q is the flow discharge, h is the flow depth, k is the geometric roughness height (range of bed elevations),  $\tau_0$  is the bed shear stress (calculated from the depth-slope product) and Re is the flow Reynolds number.

and the downstream weir was adjusted to achieve uniform depth for as large a reach as possible. The flow depth was measured using a vernier point gauge located on the flume rails. The experimental runs were divided into two phases. The first phase of the tests was designed to investigate the effect of a change in relative submergence at a single bed slope (runs 1–6 in Table 1). Different flow depths *h* were created using different flow discharges. In the second phase, experimental runs were carried out that used a combination of different flow discharges and bed slopes so that the mean bed shear stress was almost identical ( $\pm 3\%$ ) for each run (runs 6–11 in Table 1).

The use of a flume provided a number of advantages to carrying out the tests in the field: it was possible to (i) provide a more detailed spatial investigation of the near-bed flow field than would have been feasible within a gravel-bed river. This was important given that previous attempts to examine the effect of spatial variance in fluid shear stress on bedload flux have relied on theoretical distributions (Ferguson, 2003) or the assumption that the spatial distribution of flow depth can act as a suitable surrogate (Paola, 1996; Nicholas, 2000). (ii) Conduct tests at the same mean bed shear stress by using different combinations of flow depths and bed slopes. This would not have been possible within the field. (iii) Conduct tests at different bed slopes but with the same bed surface topography. Again impossible within the field.

## 2.2. Velocity measurements

A two-dimensional particle image velocimetry (PIV) system was used to provide detailed spatial measurements of fluid velocity above the gravel deposit. Many previous approaches to utilise PIV to study the hydrodynamics of flows over rough sediment boundaries have taken measurements at one lateral position across the bed by using a vertical light sheet orientated normal to the bed surface (in a vertical plane) (e.g., Campbell et al., 2005; Sambrook Smith and Nicholas, 2005; Hardy et al., 2009). A different approach was adopted here, whereby the light sheet was located parallel to the deposit surface to obtain streamwise and lateral velocities at one vertical height above the bed. This allowed velocity measurements at many more measurement locations over the deposit than is possible with the use of PIV in a vertical plane. In addition, it enabled the characterisation of the areal variability in streamwise velocities; this is important if the range of fluid drag forces on surface sediment grains are to be examined. For every experimental run, barring runs 1 and 11, PIV measurements were taken at six different heights above the bed: 3, 5, 7, 9, 11 and 18 mm above the maximum bed elevation. For run 1, heights of 11 and 18 mm were not measured because they were too close to the water surface, and for run 11, the PIV data for heights of 11 and 18 mm was lost during backup. The light sheet had a thickness of  $\sim 2$  mm so measurements were not possible closer than 3 mm to

the maximum bed elevation. This was to ensure there was no interference between the light sheet and the deposit surface. The measurements made at all the different heights will be used to analyse the velocity distributions, whereas only those at a height of 3 mm will be used for investigating the effects on bedload flux.

The cameras imaged a measurement area of  $198.4 \times 200.0$  mm<sup>2</sup> at 9.1 m from the inlet. An interrogation area of  $3.15 \times 3.15$  mm<sup>2</sup> was used in the cross-correlation of the images and allowed the flow field to be measured close to the grain scale. These areas were overlapped by 50% in both the streamwise and lateral direction. This arrangement provided 62 velocity measurements in each lateral direction and 61 measurements in each streamwise direction, and resulted in 3782 measurement locations within the image area. The flow was sampled for 5.5 min at a frequency of 9 Hz. For each PIV plane, the measurements were used to derive the time-averaged streamwise velocity  $\bar{u}$  for each of the measurement locations over the bed. This enabled the double-averaged (time and space averaged) streamwise velocity  $\langle \bar{u} \rangle$  to be calculated at a given height above the bed. The probability density functions of the distributions of  $\bar{u}/\langle \bar{u} \rangle$  will be examined, along with their statistical moments. This information will be used to describe the change in the spatial distribution of time-averaged velocity with relative submergence.

The distributions will be compared for the different hydraulic conditions at the same relative height  $z/k$ . The datum height  $z$  is the height above the maximum bed elevation (roughness crest), and  $k$  is the bed geometric roughness height (equal to the range of bed surface elevations). These estimates are derived from a laser scan of an area of bed covering the PIV measurement area. Runs are compared at the same height relative to the roughness height, rather than relative to flow depth, because previous studies have shown that the vertical change in the spatial properties of the flow scale well with  $k$  (e.g., Manes et al., 2007; Aberle et al., 2008; Cooper and Tait, 2010).

## 2.3. Modelling the effect of spatial variance on bedload flux

To investigate the effect of fluid and critical shear stress variance on bedload flux, a statistical model of bedload transport used by Ferguson (2003) is modified. It is used in three ways. First to compare the bedload flux with variance in fluid shear stress  $\tau$  and no variance in critical shear stress  $\tau_c$  to the bedload flux when both are assumed invariant. This allows the effect of variance in  $\tau$  to be isolated from the effects of variance in  $\tau_c$ . Secondly to understand how this comparison changes when variance in  $\tau_c$  is incorporated. Finally to compare the bedload flux with variance in both  $\tau$  and  $\tau_c$  to one where both are assumed invariant. This will allow the applicability of spatially averaged estimates of bedload flux to be assessed.

All approaches use the same form of equations. The total bedload flux  $Q_b$  [L<sup>3</sup> T<sup>-1</sup>] over some width  $w$  is estimated using the Meyer-Peter and Müller (1948) transport function

$$Q_b = wa \int_0^{y_{\max}} y^{1.5} p(y) dy \quad (1)$$

where  $a$  is an empirical coefficient,  $y = \tau - \tau_c$ , and  $p(y)$  is the probability density function of  $y$ . Eq. (1) is used to calculate the flux when one or both of  $\tau$  and  $\tau_c$  are set as variable. If both are assumed constant, the spatially averaged bedload flux is given by

$$\langle Q_b \rangle = wa[\langle \tau \rangle - \langle \tau_c \rangle]^{1.5} \quad (2)$$

where the angled brackets denote a spatial average.

For the first stage of the analysis  $y$  in Eq. (1) is set equal to  $\tau - \langle \tau_c \rangle$  to give the bedload flux with variable  $\tau$ , denoted by  $Q_{\tau, \langle \tau_c \rangle}$ . To compare this with flux with no variance in  $\tau$  and  $\tau_c$ , the relative flux  $Q_{\tau, \langle \tau_c \rangle}^* = Q_{\tau, \langle \tau_c \rangle} / \langle Q_b \rangle$  is examined. This means that the flux has arbitrary units such that  $Q_{\tau, \langle \tau_c \rangle}^* = 1$  when  $\tau$  is invariant and  $w$  and  $a$  can

be set to any arbitrary value. For the second stage of analysis,  $Q_b$  is compared to the flux given by setting  $y = \langle \tau \rangle - \tau_c$ , denoted by  $Q_{\langle \tau \rangle, \tau_c}$ . Here the relative flux is given by  $Q_{\tau_c}^* = Q_b / Q_{\langle \tau \rangle, \tau_c}$ . In the final stage the relative flux is given by  $Q_b^* = Q_b / \langle Q_b \rangle$ .

For the first part of the analysis the excess shear stress  $\tau - \langle \tau \rangle$  will be varied to examine how the effect of the spatial variability changes for different levels of excess shear stress. This also allows the results to be better compared with the results in [Ferguson \(2003\)](#) and to model different transport conditions. [Ferguson \(2003\)](#) identified that  $1/c = \langle \tau \rangle / \langle \tau_c \rangle$  is a dimensionless transport stage and that a gravel-bed river typically conveys most bedload when it attains a value of 1.2–1.4 (e.g., [Parker, 1978](#); [Andrews, 1984](#); [Paola, 1996](#)), implying  $c \approx 0.7$ – $0.8$ . As such, Ferguson used a  $c$  value of 0.8 to represent conditions of maximum bedload transport in a gravel-bed river. To simulate increasing amounts of sand within the bed he lowered the value of  $c$ . The present paper follows this approach using  $\langle \tau_c \rangle = c \langle \tau \rangle$  to give different (mean) levels of excess shear stress. Because a decrease in  $c$  reflects a fining of the bed surface,  $c$  is varied between 0.3 and 0.8, in which 0.8 represents the condition of maximum bedload conveyance. The lower limit is based on the following reasoning. A gravel bed with  $D_{50} = 2.00$  mm is the lower end of the size range that would normally be used to classify a gravel bed (assuming a low sand proportion within the bed) (cf. [Singer, 2008](#)). At  $c = 0.8$ , the  $D_{50}$  is 4.97 mm (the grain size of the deposit); assuming that  $\tau_c = 0.045(\rho_s - \rho)gD_{50}$ , the ratio of  $\tau_c$  for  $D_{50} = 2.00$  mm to  $\tau_c$  at  $D_{50} = 4.97$  mm is equal to 0.4. If 0.4 is multiplied by  $c = 0.8$ , this produces a lower limit of  $c = 0.3$ . This limit represents a fine gravel bed.

It is reasonable to use the same velocity spatial distributions for different  $c$  values for two reasons. Firstly, the results from the PIV measurements indicate that the degree of spatial variance in velocity is similar to the levels measured over other gravel deposits (see below). Secondly, [Sambrook Smith and Nicholas \(2005\)](#) showed that the spatial patterns of mean flow velocity and fluid stress are broadly similar for gravel beds with varying degrees of sand deposition (and therefore fining).

2.4. Estimation of fluid shear stress

The velocity data from the laboratory tests is used to estimate the spatial distribution of fluid stress. At a spatial location  $x, y$  over the bed, it is given by

$$\tau_{x,y} = 0.5\rho C_D \bar{u}_{x,y}^2 A \tag{3}$$

where  $C_D$  is the drag coefficient and  $A$  is the exposed frontal area of the sediment grains. This provides a spatial distribution of  $\tau$  over a water-worked gravel bed, rather than a lateral distribution, as modelled by [Ferguson \(2003\)](#).

Eq. (3) provides “time-averaged” shear stress values, and the model therefore captures the effects of fluid drag on bedload flux under steady state conditions. The experimental approach allows the fluid shear stress to be estimated at 3 mm above the roughness crest, at  $z/k = 0.2$ . The total fluid shear stress has an approximately linear profile within the region between this measurement height and the roughness crest for the range of studied submergences ([Cooper and Tait, 2010](#)). As such, the discrepancy between the fluid shear stress, estimated using near-bed flow velocities, and the stress experienced on the grain surface is consistent for the different experimental runs.

To compare the effects of spatial variability in  $\tau$  on bedload flux for the different experimental runs, the fluid stress distribution is scaled by its spatial mean to give the dimensionless fluid stress  $\tau^*$ . This has the added effect that  $C_D$  and  $A$  in Eq. (3) can have arbitrary values.

2.5. Estimation of critical shear stress

Measurements of  $\tau_c$  for water-worked gravel beds are rare and we are not aware of any study that has measured its full distribution. [Bottacin-Busolin et al. \(2008\)](#) performed measurements at a level of shear stress just above the critical shear stress, so they were only able to characterise the lower range of critical entrainment velocities. Instead we have simulated the distribution of  $\tau_c$  using a discrete particle model first developed by [McEwan and Heald \(2001\)](#). The model estimates the distribution of near-bed flow velocities at the threshold of motion for all surface grains. Only a brief description is provided here; further details of the model can be found in [Heald et al. \(2004\)](#). The model represented individual grains as spheres and formed a sediment deposit with the same grain size distribution used in the laboratory tests. The deposit was formed by releasing the spheres in sequence into a still fluid, each from a random position in a horizontal plane located well above the surface. Each particle fell under the influence of gravitational and fluid drag forces before it underwent a series of collisions with previously deposited particles and came to rest in a stable position. The submerged weight and the exposed area of the individual particles in the numerically deposited beds was then analysed to estimate the near-bed flow velocity that would cause the drag force to be capable of moving the individual particles exposed on the surface. This was resolved by calculating the critical value of streamwise velocity that produced a destabilising moment sufficient to overcome the stabilising moment caused by the grain’s submerged weight. Implicitly, therefore, the model accounts for the influence of grain roughness on critical shear stress. The modelled critical entrainment velocities  $u_c$  are shown in [Fig. 1](#). These are used to estimate the distribution of  $\tau_c$  through Eq. (3). The distribution is assumed to be statistically stationary. To use the DPM data for the different hydraulic conditions,  $\tau_c$  will be scaled by its spatial mean to give  $\tau_c^*$ .

The use of a drag force term is justified for two reasons. Firstly, [Schmeeckle et al. \(2007\)](#) found a strong correlation between the instantaneous drag force acting on a grain and the instantaneous streamwise velocity. This was not the case for the instantaneous velocity cross products or lift forces. Secondly, a number of studies have demonstrated that some aspect of streamwise velocity strongly correlates with sediment entrainment transport, but that the cross products of velocity have a poorer relationship with sediment entrainment ([Williams et al., 1989](#); [Clifford et al., 1991](#); [Papanicolaou et al., 2001](#)). For example, [Bottacin-Busolin et al. \(2008\)](#) discovered that over half of the grain movements observed over a gravel bed were due to variations in the streamwise component of velocity,

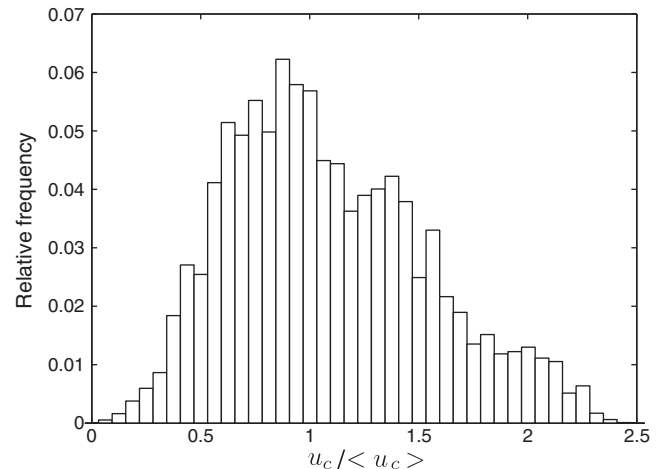


Fig. 1. The modelled distribution of critical entrainment velocities  $u_c$  scaled by their spatial mean ( $u_c$ ).

and only in a relatively small percentage of the cases (around a tenth) were they characterised by changes in the cross-product of temporal fluctuations in velocity.

### 3. Results

#### 3.1. Effect of relative submergence on the spatial distribution of flow velocity

The probability density functions of  $\bar{u}/\langle\bar{u}\rangle$  for all the experimental runs are shown in Fig. 2. This is taken from the velocity measurements made at a relative height of  $z/k=0.2$ , the lowest height above the deposit. They show the considerable spread in  $\bar{u}$ . Some areas of the bed can experience  $\bar{u}$  values as low as 60% of  $\langle\bar{u}\rangle$ , but others display values over 120% of  $\langle\bar{u}\rangle$ . Therefore some areas have values that are over two times higher than others areas. Fig. 2 also shows that the degree of spread in the values and the shape of the distributions differ between the experimental runs, varying with the value of relative submergence. This is investigated further in Figs. 3–4 by examining the moments of the distributions. These are shown at different relative heights above the bed to demonstrate the consistency of the results.

The standard deviation in  $\bar{u}$ ,  $\sigma_{\bar{u}}$  is used as a measure of the degree of spatial variance in  $\bar{u}$ . Only absolute values of standard deviation will be compared between the different runs because the interest is in quantifying the variation in shape with a change in relative

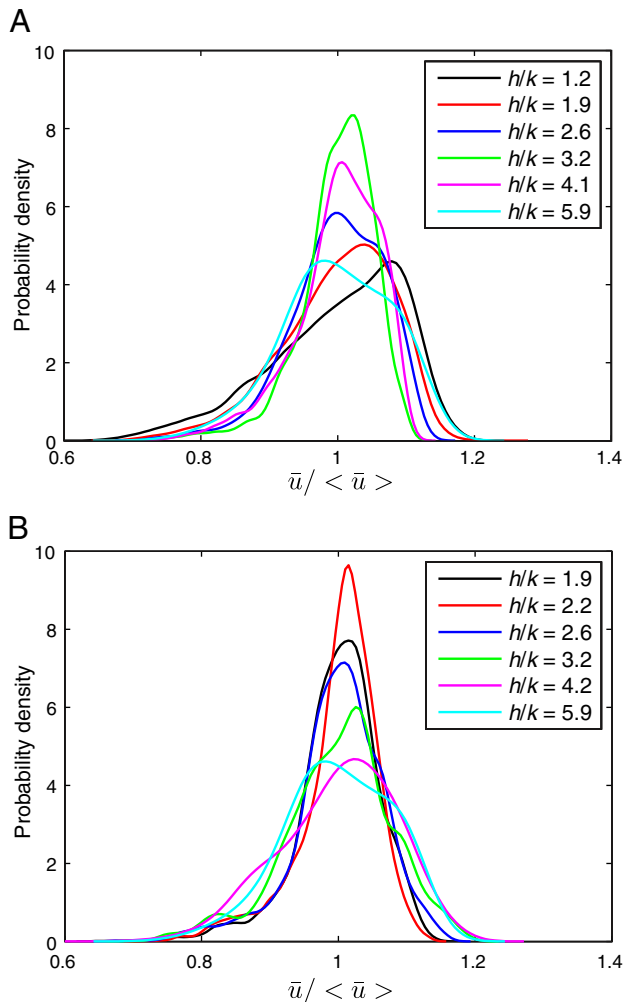


Fig. 2. Probability density functions of  $\bar{u}/\langle\bar{u}\rangle$  for the experimental runs performed at (A) a single bed slope and (B) the same mean bed shear stress at  $z/k=0.2$ .

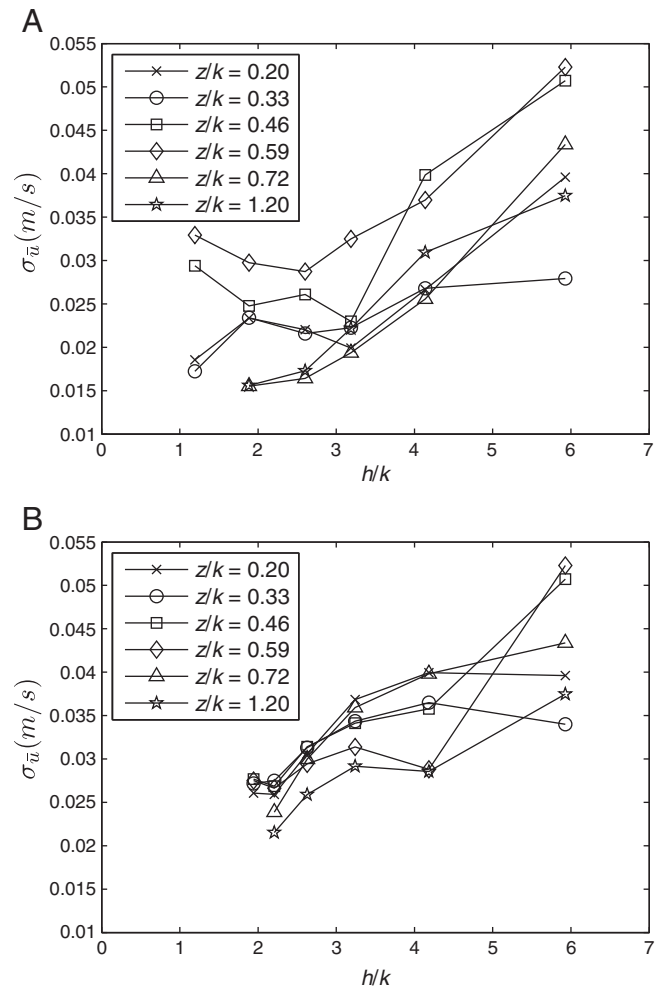


Fig. 3. The change in spatial variability in time-averaged velocity with relative submergence at various heights above the bed. This is for the experimental runs performed at (A) a single bed slope and (B) the same mean bed shear stress.

submergence. Fig. 3 reveals that, at the same values of  $z/k$ ,  $\sigma_{\bar{u}}$  displays a clear trend to increase with a rise in relative submergence.

The skewness in the distribution of  $\bar{u}$  also displays a clear change with relative submergence (Fig. 4A). As the flow becomes deeper, the distributions become less negatively skewed and more symmetrical in all but the test at the lowest submergence. This indicates that, typically, at lower submergences the flow over the bed has localised areas of distinctly low  $\bar{u}$  balanced by large areas of just slightly higher-than-average  $\bar{u}$ . As the submergence increases, the flow organisation becomes more uniform. The distributions of  $\bar{u}$  are all negatively skewed, except for one distribution that is near symmetrical (run 6 at  $z/k=1.2$ ).

Fig. 4B shows that the kurtosis of the distributions of  $\bar{u}$  also change with relative submergence. Typically distributions change from being leptokurtic at the low submergences to be near-normal in peakedness at the higher flow depths. This reflects the change in skewness, showing that the distributions tend toward the shape of a normal distribution as submergence rises. The effects of the variance and changes with submergence on bedload flux are now examined.

#### 3.2. Effect of fluid shear stress variance and relative submergence on bedload flux

In the first stage of analysis  $\tau_c$  is assumed to be invariant so that the effects of variance in  $\tau$  can be isolated. The change in  $Q_{(\tau_c)}^*$  with excess shear stress is shown in Fig. 5 for the tests at a single bed

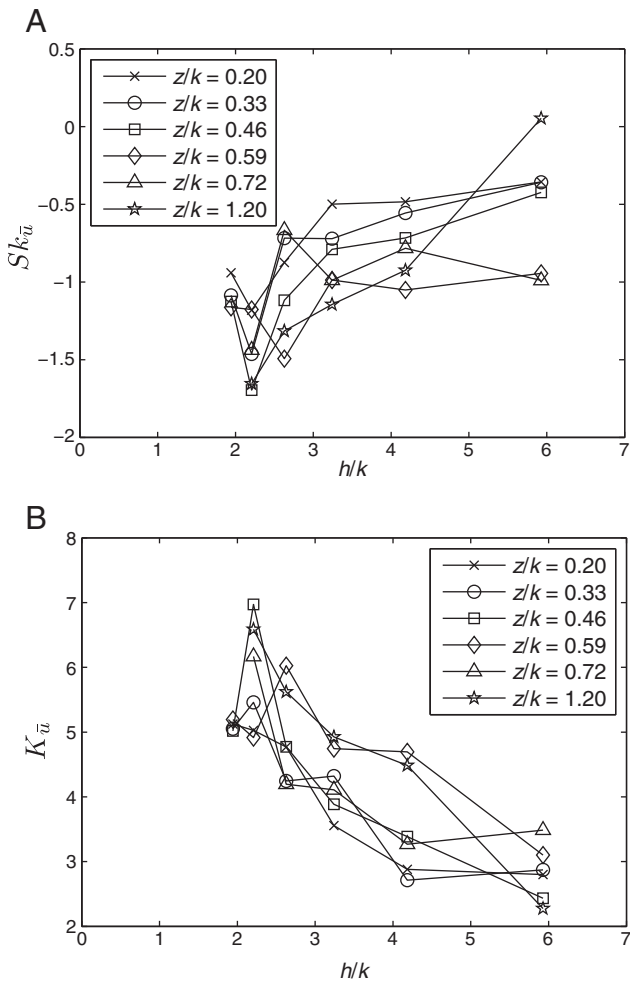


**Fig. 4.** The change in (A) skewness and (B) kurtosis of the spatial distribution of time-averaged velocity with relative submergence at various heights above the bed.

slope and those at the same mean bed shear stress. Considering the two plots together, bedload flux is greater when  $\tau$  is variant. At a low excess shear stress, bedload flux is nearly 40% higher than when  $\tau$  is invariant. This is because the increase in specific flux in areas of the bed with above-average  $\tau$  is bigger than the decrease in specific flux in parts with below-average  $\tau$ .

The relative bedload flux decreases with a rise in excess shear stress such that at a high excess, variance in  $\tau$  has little influence. It implies that its effects are more important in low transport conditions.

Now focussing on the differences in  $Q_{\langle\tau_c\rangle}^*$  between the different experimental runs, Fig. 5 shows there is an increase in flux with a rise in relative submergence both at a single bed slope and for the tests at the same mean bed shear stress. At low submergences, bedload flux can be 15% higher – but a factor of nearly 1.4 times larger at the highest submergences – than when  $\tau$  is invariant. This increase is purely attributable to changes in the probability distribution of  $\tau$ .

Relative submergence has a more noticeable influence on  $Q_{\langle\tau_c\rangle}^*$  with a decrease in excess shear stress, and has little effect at high levels of excess shear stress. This is because the variance in  $\tau$  increases with relative submergence, and this variance has a greater influence on bedload flux at the lower values of excess shear stress.

### 3.3. Effect of critical shear stress variance on bedload flux

The second stage of analysis involves examining the effect of variance in  $\tau$  when the bed has a spatial distribution of  $\tau_c$ . Fig. 6

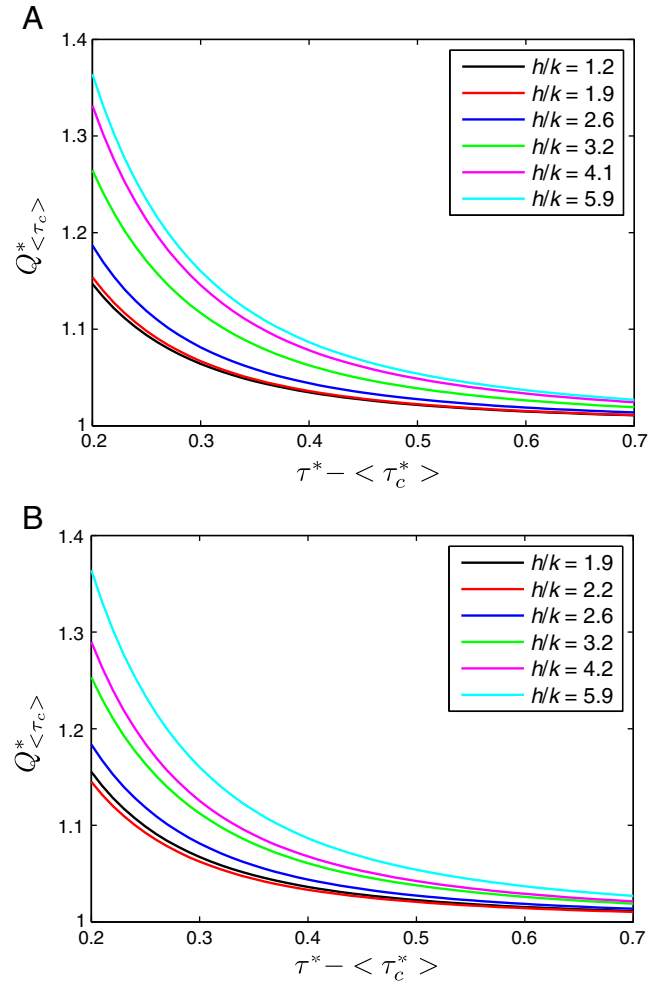


**Fig. 5.** The change in relative bedload flux with excess shear stress for the first stage of analysis when only the effects of variance in fluid shear stress are considered. This is for the experimental runs performed at (A) a single bed slope; and (B) the same mean bed shear stress.

summarises the change in  $Q_{\tau_c}^*$  with relative submergence at  $c = 0.8$ , along with  $Q_{\langle\tau_c\rangle}^*$  for comparison. Data points are plotted for experimental runs undertaken both at a single bed slope and at the same mean bed shear stress. It shows that variance in  $\tau$  now has little

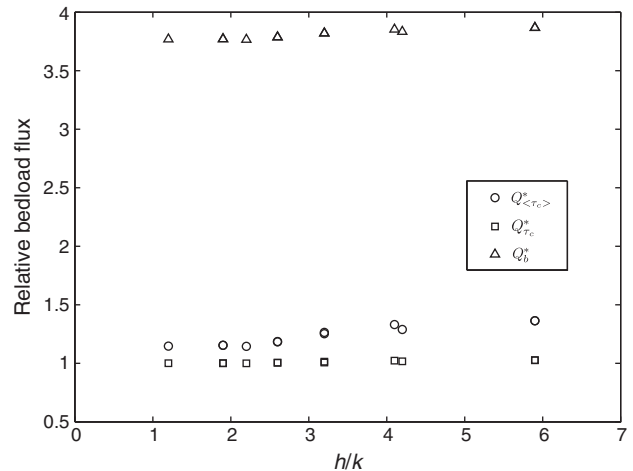


**Fig. 6.** The change in relative bedload flux with relative submergence for the three different stages of analysis. This is shown for all experimental runs at  $c = 0.8$ .

effect on bedload flux. Incorporating variance in  $\tau_c$  causes the spatial distribution of excess shear stress to be close to symmetrical; the increase in specific flux in areas of the bed with above-average  $\tau$  is only slightly larger than the decrease in specific flux in parts with below-average  $\tau$ . This is related to the shape of the distributions of  $\tau$  and  $\tau_c$ ; the former is negatively skewed and the latter is positively skewed.

For the third stage of the analysis, the effect of assuming an invariant  $\tau$  and  $\tau_c$  is sought. The  $Q_b^*$  values in Fig. 6 show bedload flux is around four times under this assumption. When compared to the values from the previous two stages of analysis, clearly spatial variability in  $\tau_c$  has a much larger effect than variance in  $\tau$ . This is because the spread of the distribution of  $\tau_c$  is much higher than that of  $\tau$  (see Figs. 1 and 2). The increased bedload flux, caused by variance in  $\tau$  and  $\tau_c$ , is therefore primarily because the reduction in flux from the more stable grains is significantly less than the increase in flux from the less stable grains. This is caused by the positive skewness of the distribution of  $\tau_c$ .

The bedload flux shows the same trend observed earlier, increasing with relative submergence. This is a consistent trend, demonstrated by the overlapping of data points at the same levels of submergence but at different bed slopes. The differences between  $Q_{\tau_c}^*$  and  $Q_b^*$  reduce slightly with a rise in submergence. This indicates that the effects of variance in  $\tau_c$  become slightly less important compared to the effects of variance in  $\tau$  at higher submergences (because variance in  $\tau$  rises with submergence).

## 4. Discussion

### 4.1. Spatial distribution of flow velocity

The velocity measurements revealed that the near-bed velocity distribution had a number of characteristics that closely matched those found both in gravel-bed rivers and other gravel beds in laboratory flumes. First, the results revealed that the degree of spatial variability in flow velocity increases with relative submergence. This was shown to be consistent throughout the flow. This is the same trend observed by Clifford (1996) in a gravel-bed river, and the degree of increase in  $\sigma_{\bar{v}}$  with submergence is very similar to that predicted by the regression model of Buffin-Bélanger et al. (2006) for a water-worked gravel-bed surface in a laboratory flume. In the laboratory tests in the current paper, an increase in relative submergence corresponds with an increase in Reynolds number (see Table 1). As such, it shows that  $\sigma_{\bar{v}}$  also increases with a rise in Reynolds number, and this supports the laboratory observations of Hardy et al. (2009) for a water-worked gravel bed. Secondly, the degree of velocity variance compares favourably with those reported by field studies in gravel-bed rivers (Smart, 1999; Byrd et al., 2000; Roy et al., 2004). Thirdly, the skewness and kurtosis values for the distribution of velocity revealed that the probability distributions tend toward the shape of a normal distribution as the flow became deeper. This supports the observations of Legleiter et al. (2007) who found that the spatial structure of time-averaged velocity became more uniform with a rise in flow depth as the bed particles became increasingly drowned out. And also those of Lamarre and Roy (2005) who concluded that the distribution of the mean flow properties displayed a well-organised, coherent spatial pattern that was controlled by flow depth. The distribution shapes are also similar to those reported for other gravel beds (Barison et al., 2003; Cooper and Tait, 2009). Finally, all these results support the conclusions of others that flow depth is an important control on flow structure over water-worked gravel beds (Roy et al., 2004; Lamarre and Roy, 2005; Legleiter et al., 2007). Overall this reveals that the trends that have been observed in the laboratory tests are consistent with results where both grain and form roughness effects are present, and the flow has a spatial distribution that resembles features found over other gravel beds. This

provides assurance that it was appropriate to use this data in the bedload model.

### 4.2. Effect of fluid shear stress variance

At the grain scale, variance in  $\tau$  only had an appreciable influence on bedload flux when the bed was assumed to have no variance in  $\tau_c$ , when levels of excess shear stress were low, and when the flow had a high relative submergence. It had a negligible influence when the bed had a spatial distribution of  $\tau_c$ . Its largest influence was observed through its effect on the variation in bedload flux with relative submergence.

To compare these results to those of Ferguson (2003), who used a statistical model of  $\tau$ , a consideration must be made of the degree of spatial variance simulated in his study. He assumed shear stress to be below its mean value  $r$  in a proportion  $p$  of the total channel width and to vary randomly between 0 and  $r$  within  $p$ . The spatial variability in  $\tau$  was equal to  $r^2p/3(1-p)$ , and the influence of this spatial variability on bedload flux was investigated by varying the parameter  $p$ , which was used as a stress variance index and accounted for changes in channel planform. For sake of comparison, the  $p$  values for the PIV data can be estimated by examining the proportion of the distribution where  $\tau < \langle \tau \rangle$ . This was found to range from 0.36 to 0.54 and corresponds well with Ferguson's thought that low values of  $p$  correspond to flume-like conditions. For a  $p$  value of 0.5, the fluid shear stress was simulated by Ferguson (2003) to be distributed uniformly across the channel width between 0 and  $2\langle \tau \rangle$ , so any direct comparisons are difficult. Nonetheless at  $c = 0.8$  and with a constant  $\tau_c$ , he found a threefold increase in bedload conveyance compared to flows with no variance in  $\tau$ . Paola (1996) and Nicholas (2000) applied their model to measurements from a laboratory-scaled model of a braided river and from a braided river in New Zealand for comparable conditions, in which they also assumed a spatially averaged value of  $\tau_c$ . Paola (1996) found that the increase was a factor of  $\sim 3$ , and Nicholas (2000) discovered a range of two to three. At similar  $p$  values and  $c = 0.8$  the increase in bedload flux from the velocity data is around half of that found by these previous studies.

The results from the laboratory showed that the effect of variance in  $\tau$  on bedload flux increased with a lowering in excess shear stress. This supports the conclusions of Nicholas (2000), in which the fluxes estimated with and without  $\tau$  variance also converged at the highest bedload transport rates. Overall, these comparisons suggest that flow variance caused by grain roughness has the same, but reduced, effect on bedload flux as when high levels of form roughness are present.

### 4.3. Effect of critical shear stress variance on bedload flux

The results reveal that variance in  $\tau_c$  has a much larger influence on bedload flux than variance in  $\tau$ . This is revealed through three observations. First, when the analysis was repeated for the deposit used in the flume, which had a spatial distribution of  $\tau_c$ , the effects of variance in  $\tau$  on bedload flux were negligible. Bedload flux was only a few percent higher than when  $\tau$  was invariant. Ferguson (2003) examined the influence of bed patchiness on bedload flux for different scenarios, one of which was the effect of random patchiness, which most closely simulated the influence of grain roughness. His results also show a diminished effect. For example, at a  $p$  value of 0.5 and  $c = 0.8$  his results revealed that the bedload flux increase is only around half of what it was when the bed was assumed to have no variance in  $\tau_c$ .

Secondly, bedload flux was around four times higher when both  $\tau$  and  $\tau_c$  was variant, and it was only 15–40% higher when only  $\tau$  was variant. A similar, but reduced effect, was also observed by Ferguson (2003). At a  $p$  value of 0.5, his results showed that bedload flux was around 4–5 times higher with a variance in both – a very similar

magnitude to the laboratory results – and about 3 times higher with just a variance in  $\tau$ .

Finally, spatial variability in  $\tau_c$  caused bedload flux to be much higher. Bedload conveyance was around three times higher than when the bed was assumed to have no variance in  $\tau_c$ . At a  $p$  value of 0.5, Ferguson (2003) found the increase to be around 100–200%.

Overall then, variance in  $\tau_c$  is observed to have a similar but larger effect on bedload flux in the laboratory tests than simulated by Ferguson (2003), even though the effects of grain roughness are only considered. This is because of a difference in the spread of the distributions. Ferguson (2003) simulated  $\tau_c$  to vary symmetrically by  $\pm 50\%$  and  $\pm 100\%$  around its mean value, producing a different distribution shape to the one simulated by the DPM. The DPM distribution had a much greater spread and a positively skewed shape (see Fig. 1) that acted to make its influence greater. It suggests that Ferguson (2003) underestimated the effects of form roughness on the distribution of  $\tau_c$ , or that grain roughness effects are greater than commonly acknowledged.

#### 4.4. Effect of relative submergence on bedload flux

The changes in the spatial distribution of  $\tau$  caused the bedload flux to increase with a rise in relative submergence. This increase was a consistent trend regardless of whether  $\tau_c$  was variant or not. It occurred for flows at the same bed slope as well as at different bed slopes, and at the same submergence, the bedload flux was almost identical. This supports the thought that a reduction in river width will, with other things being equal, lead to an increase in bedload transport. The changes with relative submergence are, however, more minor in comparison to those caused by variance in  $\tau_c$ .

The effects of relative submergence were also slightly reduced when  $\tau_c$  was variant. Given that variance in  $\tau$  increased with relative submergence, this matches the pattern predicted by Ferguson (2003). He found bedload flux to rise more considerably with an increase in variance in  $\tau$  for a bed with invariant  $\tau_c$ .

A number of studies have highlighted that the mean bed shear stress at which sediment is entrained is positively correlated to channel slope (e.g., Ashida and Bayazit, 1973; Bathurst et al., 1983, 1987; Shvidchenko and Pender, 2000; Mueller et al., 2005; Pender et al., 2007; Lamb et al., 2008; Parker et al., 2011). Several arguments have been used to explain this relationship: in steeper rivers increased channel form roughness is present (Petit et al., 2005), stabilising bed structures and hiding effects are more prominent (Mueller et al., 2005), and flow aeration occurs (Wittler and Abt, 1995). None of these completely account for the effect of slope. The critical shear stress is still positively related to slope in flows where form roughness is low (Shvidchenko and Pender, 2000; Mueller et al., 2005; Parker et al., 2011), and the effect of slope is not caused by increased drag from channel walls and morphologic structures (Lamb et al., 2008).

Numerous studies have suggested that the reduced mobility on steep slopes can be attributed to a lower relative submergence  $h/k$  (e.g., Buffington and Montgomery, 1997; Shvidchenko and Pender, 2000; Mueller et al., 2005; Lamb et al., 2008; Parker et al., 2011). The results in the present paper confirm this. Bedload flux increased with a rise in submergence at a constant bed slope and over a bed with the same spatial distribution of  $\tau_c$ , which exhibited only grain roughness. Slope had an indirect effect.

Previous studies have hypothesised that the correlation between mobility and submergence arises because a lower relative submergence causes a decrease in local flow velocity around bed particles (Ashida and Bayazit, 1973; Graf, 1991; Lamb et al., 2008). Shvidchenko and Pender (2000) suggested this is caused by the increased effect of wake eddies shed from bed particles at higher slopes on the overall flow resistance. Lamb et al. (2008) demonstrate, using a one-dimensional force balance model, that the decrease in local

flow velocity is caused by a change in eddy viscosity (induced by the wakes) and not by a reduction in fluid stress caused by increased grain-induced fluid drag.

The results in the present paper partially support this hypothesis. The results revealed that with the same distribution of  $\tau_c$  and the same mean  $\tau$  (which was a result of grain-induced fluid drag) an increase in bedload flux with submergence still occurred. The increase was attributable purely to changes in the spatial distribution of  $\tau$ . These reflect a change in the distribution, rather than an overall lowering, of local near-bed flow velocity at the grain scale.

#### 4.5. Implications for bedload modelling

The findings have a number of implications for bedload sampling, but the focus here will be on their implications for predicting bedload transport. The results have revealed that, even for beds where just grain roughness dominates, if  $\tau_c$  is assumed to be constant, the bedload flux will be severely underestimated by a one-dimensional model of bedload flux. However, a spatially averaged estimate of  $\tau$  may be sufficient to achieve accurate calculations for water-worked sediment beds that have variance in  $\tau_c$ . However smaller but significant errors do arise because of variance in  $\tau$  when the bed has no variance in  $\tau_c$ . The implication is that one-dimensional estimates of bedload flux should not be used in the design of irregular, artificial channels. Because of the correlation between bedload flux and relative submergence, one-dimensional estimates will be less accurate in wider channels and in higher flows.

Overall, the work suggests that the concept that bedload transport models can be calibrated by mean bed shear stress and applied across a range of submergences (e.g., during a flood) is a flawed one. It is the spatial distribution of excess shear stress that is important, and this will depend on the spatial organisation of  $\tau$  (which is influenced by the level of relative submergence) and  $\tau_c$  (which will presumably depend on the bed surface topography). A more complete understanding on how the spatial variance in  $\tau$  and  $\tau_c$  affect bedload flux, and how we might correct spatially averaged estimates, will require covering a wider range and more diverse conditions than studied here. A number of questions therefore still remain. How do the spatial patterns of  $\tau$  and  $\tau_c$  change with different roughness scales (and different combinations thereof), from patch to patch, section to section of rivers, and between rivers of different geometries? One could speculate that for sinuous channels where form roughness dominates, the spatial variance in  $\tau$  and  $\tau_c$  is likely to be higher and the discrepancy between modelled and measured fluxes will be greater. This suggests it will be problematic to apply the same parameterised bedload transport model to different flow, bed, and channel conditions.

Thus, the spatial distributions of  $\tau$  and  $\tau_c$  need to be incorporated into bedload transport models for a given channel condition, not only to account for their variance but also the change in shape of  $\tau$  with relative submergence. Presently we know very little about the shape of the spatial distributions, let alone how they may vary in time during active transport. Efforts are required to estimate/measure spatial distributions of  $\tau$  and  $\tau_c$  to arrive at a fuller assessment of the influence of spatial variance in  $\tau$  and  $\tau_c$  on bedload flux and to understand the best way to incorporate their effects within bedload transport models. There are two issues that need to be resolved if this is to occur:

- Traditionally, the estimation of bed shear stress in rivers usually involves either (i) the assumption of steady, uniform flow and the extrapolation to the bed of a linear vertical stress profile; (ii) the extrapolation of a vertical velocity profile down to the roughness trough and then the use of empirical drag/roughness coefficients to estimate a value of shear stress; or (iii) the use of the locally measured, time-averaged Reynolds stress extrapolated to the bed. All these methods either suffer from very restrictive assumptions,



ignore the spatial complexity of gravel beds, or rely on site-specific coefficients. They are often only able to evaluate a spatially and/or temporally averaged shear stress and not at an individual grain or pore level. The present paper has used spatially distributed velocity measurements to estimate  $\tau$  through a drag force equation. Although these measurements are at the grain scale, it is not ideal because the fluid shear stress above the bed differs from the shear stress acting directly on the surface of a grain. Presently no methods exist to evaluate directly boundary shear stress. Spatially distributed measurements within the roughness layer are required (see Cooper and Tait, 2010) over surfaces with different topographies so we can evaluate/parameterise the link between bed geometry and shear stress organisation.

- The author is not aware of any study that has been able to characterise fully the spatial distribution of  $\tau_c$  for a gravel bed. This is a more acute problem because the results reveal that variability in  $\tau_c$  has a larger effect on bedload flux. It has not been possible to validate the DPM simulations against observed data. Even to just explore the effects of grain roughness, grain-scale, simultaneous and co-located measurements of  $\tau$ , bed surface topography and grain displacement over a wide range of  $\tau/\tau_c$  ratios are required. The nature of the link between bed surface topography and grain-scale  $\tau_c$  has still not been examined despite modelling studies suggesting a strong link (see Measures and Tait, 2008). This data is required to parameterise transport models.

#### 4.6. Implications for bed evolution

With all other things constant, spatial variability in  $\tau$  and  $\tau_c$  will cause variance in bedload flux even when just grain roughness is present. At the grain scale it offers partial explanation as to why beds without any notable form roughness elements become armoured. One can speculate that grain roughness will be sufficient to create a sufficient degree of spatial variance in flux to promote spatially non-synchronous sediment motion and size-selective transport.

Now consider the effects of a flood on bed evolution at the grain scale. If the effects of relative submergence on flux during a flood are first put to one side, previous studies show that as a bed becomes armoured, the standard deviation in bed elevations increases (Pender et al., 2001; Mao et al., 2011). It is likely that the variance in  $\tau_c$  is correlated with the variance in elevation, so the variance in  $\tau_c$  will also increase. Barison et al. (2003) showed, albeit with a limited data set, that the trend is for the distributions of near-bed, time-averaged velocities to also become more variable as the bed armours, and so causing an increase in the variance in  $\tau$ . This leads one to speculate that variance in bedload flux will increase during armouring, reflecting the fact that entrainment becomes more size and spatially selective.

If the effects of relative submergence are added in to this scenario, during the rising limb the flux will be enhanced, along with the pace of degradation, relative to the increase in flux that normally occurs with an increase in bed shear stress. During the falling limb, the decrease in submergence will have a lowering effect on flux and cause a lessening in the pace of aggradation. However, because only significant vertical sorting of sediment is likely to occur during the falling limb of the hydrograph (Hassan et al., 2006) and the effects of bed surface material changes on flux are greater, one can speculate that relative submergence will only have a noticeable effect during the rising limb.

Although the experimental design limited the study to examining grain roughness effects, a consideration of the influence of the results on large-scale bed evolution in gravel-bed rivers is worthwhile. This appears reasonable given that the results in the present paper matched the trends observed by Paola (1996), Nicholas (2000) and Ferguson (2003). One-dimensional sediment routing models (SRMs), which use width-averaged estimates of  $\tau$  and  $\tau_c$ , are commonly used to model bed evolution (e.g., Hoey and Ferguson, 1994;

Wong and Parker, 2006). Because the results in the present paper show that the level of underestimation made by one-dimensional calculations varies with excess shear stress and relative submergence, it is also likely to vary from section to section in most rivers. Therefore, not only will SRMs misrepresent the pace of aggradation or degradation, they will also misrepresent its pattern. This will influence the ability of an SRM to simulate the longitudinal patterns of change in bed elevation and the associated fining or coarsening.

## 5. Conclusions

A simple, statistical bedload model has been used to examine the effect of variance in fluid and critical shear stress on bedload flux over a water-worked gravel deposit. This was achieved by gaining estimates of spatially distributed fluid shear stress from laboratory measurements of near-bed flow velocity and simulating the distribution of critical shear stress using a DPM of the sediment distribution used in the laboratory. Only grain roughness effects on the variance in fluid and critical shear stress were considered. The velocity data were used to describe the change in the spatial distribution of near-bed velocity with relative submergence, which allowed the effects of submergence on flux to also be considered. These are the main conclusions:

- (i) Spatial variance in fluid shear stress, because of variance in near-bed velocity, only caused an appreciable increase in bedload flux when the bed was assumed to have no variance in critical shear stress. It was much lower than has been observed by other studies in conditions where form roughness was high.
- (ii) The variance in fluid shear stress, caused by grain roughness, was not sufficient to have an appreciable effect on bedload flux over water-worked beds with a spatial distribution of critical shear stress.
- (iii) Spatial variance in critical shear stress, caused by grain roughness, had a much larger influence than variance in fluid shear stress on bedload flux. It increased bedload flux by nearly 400%. This was a similar level of increase observed in studies where form roughness was high.
- (iv) The spatial variance in near-bed velocity increased and the spatial probability distributions tended toward the shape of a normal distribution with a rise in relative submergence. This occurred when the surface topography was invariant.
- (v) A rise in relative submergence caused an increase in bedload flux. This was because of changes in conclusion (iv) and not because of a lowering in the local flow velocity as has been suggested by previous studies.
- (vi) Spatially averaged estimates of fluid and critical shear stress should not be used to estimate bedload flux, even if form roughness is low. Their spatial distributions need to be incorporated into bedload transport models, not only to account for their variance but also the change in the shape of the distribution of fluid shear stress with relative submergence.

## Acknowledgements

I thank Simon Tait for providing access to the laboratory facilities, guidance on experimental design, numerous discussions, and comments on an early draft of this paper. Thanks also to Luca Mao for reading an early draft and improving its clarity, and two anonymous reviewers for helpful comments.

## References

- Aberle, J., Koll, K., Dittrich, A., 2008. Form induced stresses over rough gravel-beds. *Acta Geophysica* 56 (3), 584–600.
- Andrews, E.D., 1984. Bed-material entrainment and hydraulic geometry of gravel-bed rivers in Colorado. *Geological Society of America Bulletin* 95 (3), 371–378.

- Ashida, K., Bayazit, M., 1973. Initiation of motion and roughness of flows in steep channels. Proceedings of the 15th Congress of the International Association for Hydraulic Research, Istanbul, Turkey. Int. Assoc. Hydraul. Res. Madrid, Spain, pp. 475–484.
- Barison, S., Chegini, A., Marion, A., Tait, S.J., 2003. Modifications in near bed flow over sediment beds and the implications for grain entrainment. Proceedings of the 30th Congress of the International Association for Hydraulic Research, Thessaloniki, Greece. Int. Assoc. Hydraul. Res. Madrid, Spain, pp. 509–516.
- Bathurst, J.C., Graf, W.H., Cao, H.H., 1983. Initiation of sediment transport in steep channels with coarse bed material. In: Sumer, B.M., Müller, A. (Eds.), *Mechanics of Sediment Transport*. A.A. Balkema, Brookfield, VT, pp. 207–213.
- Bathurst, J.C., Graf, W.H., Cao, H.H., 1987. Bed load discharge equations for steep mountain rivers. In: Thorne, C.R., Bathurst, J.C., Hey, R.D. (Eds.), *Sediment Transport in Gravel-Bed Rivers*. John Wiley & Sons, New York, NY, pp. 453–477.
- Bottacin-Busolin, A., Tait, S.J., Marion, A., Chegini, A., Tregnaghi, M., 2008. Probabilistic description of grain resistance from simultaneous flow field and grain motion measurements. *Water Resources Research* 44 (9). doi:10.1029/2007WR006224.
- Buffin-Bélanger, T., Rice, S., Reid, I., Lancaster, J., 2006. Spatial heterogeneity of near-bed hydraulics above a patch of river gravel. *Water Resources Research* 42. doi:10.1029/2005WR004070.
- Buffington, J.M., Montgomery, D.R., 1997. A systematic analysis of eight decades of incipient motion studies, with special reference to gravel-bedded rivers. *Water Resources Research* 33 (8), 1993–2029.
- Buffington, J.M., Dietrich, W.E., Kirchner, J.W., 1992. Friction angle measurements on a naturally formed gravel streambed: implications for critical boundary shear-stress. *Water Resources Research* 28 (2), 411–425.
- Byrd, T.C., Furbish, D.J., Warburton, J., 2000. Estimating depth-averaged velocities in rough channels. *Earth Surface Processes and Landforms* 25 (2), 167–173.
- Campbell, L., McEwan, I., Nikora, V., Pokrajac, D., Gallagher, M., Manes, C., 2005. Bed-load effects on hydrodynamics of rough-bed open-channel flows. *Journal of Hydraulic Engineering ASCE* 131 (7), 576–585.
- Clifford, N.J., 1996. Morphology and stage-dependent flow structure in a gravel-bed river. In: Ashworth, P.J., Bennett, S.J., Best, J.L., McLelland, S.J. (Eds.), *Coherent Flow Structures in Open Channels*. John Wiley & Sons, Chichester, UK, pp. 545–566.
- Clifford, N.J., McClatchey, J., French, J.R., 1991. Measurements of turbulence in the benthic boundary-layer over a gravel bed and comparison between acoustic measurements and predictions of the bedload transport of marine gravels. *Sedimentology* 38 (1), 161–166.
- Cooper, J.R., Tait, S.J., 2008. The spatial organisation of time-averaged streamwise velocity and its correlation with the surface topography of water-worked gravel beds. *Acta Geophysica* 56 (3), 614–641.
- Cooper, J.R., Tait, S.J., 2009. Water-worked gravel beds in laboratory flumes – a natural analogue? *Earth Surface Processes and Landforms* 34 (3), 384–397.
- Cooper, J.R., Tait, S.J., 2010. Examining the physical components of boundary shear stress for water-worked gravel deposits. *Earth Surface Processes and Landforms* 35 (10), 1240–1246.
- Ferguson, R.L., 2003. The missing dimension: effects of lateral variation on 1-D calculations of fluvial bedload transport. *Geomorphology* 56 (1–2), 1–14.
- Graf, W.H., 1991. Flow resistance over a gravel: its consequences on initial sediment movement. In: Armanini, A., Di Silvio, G. (Eds.), *Fluvial Hydraulics in Mountain Regions*. Springer-Verlag, Berlin, Germany, pp. 17–32.
- Grass, A.J., Mansour-Tehrani, M., 1996. Generalized scaling of coherent bursting structures in the near-wall region of turbulent flow over smooth and rough boundaries. In: Ashworth, P.J., Bennett, S.J., Best, J.L., McLelland, S.J. (Eds.), *Coherent Flow Structures in Open Channels*. John Wiley & Sons, Chichester, UK, pp. 40–61.
- Hardy, R.J., Best, J.L., Lane, S.N., Carbonneau, P.E., 2009. Coherent flow structures in a depth-limited flow over a gravel surface: the role of near-bed turbulence and influence of Reynolds number. *Journal of Geophysical Research* 114. doi:10.1029/2007JF000970.
- Hassan, M.A., Egozi, R., Parker, G., 2006. Experiments on the effect of hydrograph characteristics on vertical grain sorting in gravel bed rivers. *Water Resources Research* 42 (9).
- Heald, J., McEwan, I., Tait, S., 2004. Sediment transport over a flat bed in a unidirectional flow: simulations and validation. *Philosophy Transactions Royal Society A* 362 (1822), 1973–1986.
- Hoey, T.B., Ferguson, R., 1994. Numerical-simulation of downstream fining by selective transport in gravel-bed rivers: model development and illustration. *Water Resources Research* 30 (7), 2251–2260.
- Kirchner, J.W., Dietrich, W.E., Iseya, F., Ikeda, H., 1990. The variability of critical shear stress, friction angle, and grain protrusion in water-worked sediments. *Sedimentology* 37 (4), 647–672.
- Lamarre, H., Roy, A.G., 2005. Reach scale variability of turbulent flow characteristics in a gravel-bed river. *Geomorphology* 68 (1–2), 95–113.
- Lamb, M.P., Dietrich, W.E., Venditti, J.G., 2008. Is the critical Shields stress for incipient sediment motion dependent on channel-bed slope? *Journal of Geophysical Research* 113 (F2). doi:10.1029/2007JF000831.
- Lawless, M., Robert, A., 2001. Scales of boundary resistance in coarse-grained channels: turbulent velocity profiles and implications. *Geomorphology* 39 (3–4), 221–238.
- Legleiter, C.J., Phelps, T.L., Wohl, E.E., 2007. Geostatistical analysis of the effects of stage and roughness on reach-scale spatial patterns of velocity and turbulence intensity. *Geomorphology* 83 (3–4), 322–345.
- Manes, C., Pokrajac, D., McEwan, I., 2007. Double-averaged open-channel flows with small relative submergence. *Journal of Hydraulic Engineering ASCE* 133 (8), 896–904.
- Mao, L., Cooper, J.R., Frostick, L.E., 2011. Grain size and topographical differences between static and mobile armour layers. *Earth Surface Processes and Landforms* 36 (10), 1321–1334.
- McEwan, I., Heald, J., 2001. Discrete particle modeling of entrainment from flat uniformly sized sediment beds. *Journal of Hydraulic Engineering ASCE* 127 (7), 588–597.
- Measures, R., Tait, S., 2008. Quantifying the role of bed surface topography in controlling sediment stability in water-worked gravel deposits. *Water Resources Research* 44 (4). doi:10.1029/2006WR005794.
- Meyer-Peter, E., Müller, R., 1948. Formulas for bed-load transport. Proceedings of the 2nd Meeting of the International Association for Hydraulic Structures Research, Stockholm, Sweden. Int. Assoc. for Hydraul. Struct. Res. Madrid, Spain, pp. 39–64.
- Mignot, E., Barthelemy, E., Hurther, D., 2009. Double-averaging analysis and local flow characterization of near-bed turbulence in gravel-bed channel flows. *Journal of Fluid Mechanics* 618, 279–303.
- Mueller, E.R., Pitlick, J., Nelson, J.M., 2005. Variation in the reference shields stress for bed load transport in gravel-bed streams and rivers. *Water Resources Research* 41 (4). doi:10.1029/2004WR003692.
- Nicholas, A.P., 2000. Modelling bedload yield in braided gravel bed rivers. *Geomorphology* 36 (1–2), 89–106.
- Paola, C., 1996. Incoherent structure: turbulence as a metaphor for stream braiding. In: Ashworth, P.J., Bennett, S.J., Best, J.L., McLelland, S.J. (Eds.), *Coherent Flow Structures in Open Channels*. John Wiley & Sons, Chichester, UK, pp. 705–723.
- Papanicolaou, A.N., Diplas, P., Dancy, C.L., Balakrishnan, M., 2001. Surface roughness effects in near-bed turbulence: implications to sediment entrainment. *Journal of Engineering Mechanics ASCE* 127 (3), 211–218.
- Parker, G., 1978. Self-formed straight rivers with equilibrium banks and mobile bed: part 2. The gravel-bed river. *Journal of Fluid Mechanics* 89, 127–146.
- Parker, C., Clifford, N.J., Thorne, C.R., 2011. Understanding the influence of slope on the threshold of coarse grain motion: revisiting critical stream power. *Geomorphology* 126 (1–2), 51–65.
- Pender, G., Hoey, T.B., Fuller, C., McEwan, I.K., 2001. Selective bedload transport during the degradation of a well sorted graded sediment bed. *Journal of Hydraulic Research* 39 (3), 269–277.
- Pender, G., Shvidchenko, A.B., Chegini, A., 2007. Supplementary data confirming the relationship between critical Shields stress, grain size and bed slope. *Earth Surface Processes and Landforms* 32 (11), 1605–1610.
- Petit, F., Gob, F., Houbrechts, G., Assani, A.A., 2005. Critical specific stream power in gravel-bed rivers. *Geomorphology* 69 (1–4), 92–101.
- Roy, A.G., Buffin-Bélanger, T., Lamarre, H., Kirkbride, A.D., 2004. Size, shape and dynamics of large-scale turbulent flow structures in a gravel-bed river. *Journal of Fluid Mechanics* 500, 1–27.
- Sambrook Smith, G.H., Nicholas, A.P., 2005. Effect on flow structure of sand deposition on a gravel bed: results from a two-dimensional flume experiment. *Water Resources Research* 41 (10). doi:10.1029/2004WR003817.
- Schmeeckle, M.W., Nelson, J.M., Shreve, R.L., 2007. Forces on stationary particles in near-bed turbulent flows. *Journal of Geophysical Research* 112 (F02003). doi:10.1029/2006JF000536.
- Shvidchenko, A.B., Pender, G., 2000. Flume study of the effect of relative depth on the incipient motion of coarse uniform sediments. *Water Resources Research* 36 (2), 619–628.
- Shvidchenko, A.B., Pender, G., 2001. Macroturbulent structure of open-channel flow over gravel beds. *Water Resources Research* 37 (3), 709–719.
- Singer, M.B., 2008. Downstream patterns of bed material grain size in a large, lowland alluvial river subject to low sediment supply. *Water Resources Research* 44 (12). doi:10.1029/2008WR007183.
- Smart, G.M., 1999. Turbulent velocity profiles and boundary shear in gravel bed rivers. *Journal of Hydraulic Engineering ASCE* 125 (2), 106–116.
- Wiberg, P.L., Smith, J.D., 1987. Calculations of the critical shear-stress for motion of uniform and heterogeneous sediments. *Water Resources Research* 23 (8), 1471–1480.
- Williams, J.J., Thorne, P.D., Heathershaw, A.D., 1989. Measurements of turbulence in the benthic boundary-layer over a gravel bed. *Sedimentology* 36 (6), 959–971.
- Wittler, R.L., Abt, S.R., 1995. Shields parameter in low submergence or steep flows. In: Thorne, C.R., Abt, S.R., Barends, F.B.J., Maynard, S.T., Pilarczyk, K.W. (Eds.), *River, Coastal and Shoreline Protection: Erosion Control Using Riprap and Armourstone*. John Wiley & Sons, New York, NY, pp. 93–101.
- Wong, M., Parker, G., 2006. One-dimensional modeling of bed evolution in a gravel bed river subject to a cycled flood hydrograph. *Journal of Geophysical Research* 111 (F3). doi:10.1029/2006JF000478.